Influence of the sagittal lumbar parameters on the stress-strain state of the spinal motor segments at transpedicular fixation

O. O. Barkov [1], O. V. Veretelnik [2], M. M. Tkachuk [2], M. A. Tkachuk [2], V. V. Veretelnik [2]

[1] Sytenko Institute of Spine and Joint Pathology National Academy of Medical Sciences of Ukraine, Kharkiv
[2] National Technical University «Kharkiv Polytechnic Institute». Ukraine

Objective. To study the stress-strain state of the elements of the human lumbar spine when we use the transpedicular system, taking into account different angular values of segmental and total lumbar lordosis. Methods. For computer modeling of the stress-strain state of the elements of the human lumbar spine after mono- and polysegmental fixation, the Workbench product was used, and for the construction of parametric three-dimensional geometric models — the SolidWorks computer-aided design system was used. 4 groups of decisions were studied, which differed in angular values of segmental and total lumbar lordosis. In each group, 11 models were analyzed that describe the lumbar segments after mono- and polysegmental fixation in various configurations of the sagittal alignment of the lumbar spine. Results. It was found that the maximum stress on the cortical bone is concentrated on the base of the L_V in case of the «pathological» intervertebral disc L_V–S in the group of patients with hyperlordosis. At polysegmental fixation of the L_I–S, there is a redistribution of stress on the cortical bone of all vertebrae, the maximum values of which is present in the bodies of the L_V and S vertebrae. And only in the group with hypolordosis this stress is minimal. The maximum stress was always on the overlying intervertebral disc during transpedicular fixation. Significant increasing of cartilage stress in the facet joints of the L_{IV}–L_V segment was recorded during fixation of the L_V–S segment in case of hyperlordosis. The maximum stress on the rods was identified in the group of patients with hyperlordosis and polysegmental fixation of the L_I–S, on screws — on L_V, L_{IV}, L_{III} vertebrae during fixation in all groups, except for hypolordosis. Conclusions. Increasing in angular values (hyperlordosis), which describe segmental and total lumbar lordosis, leads to the stress elevation in the fixing elements and structures of the spinal motor segments, and, conversely, a decreasing in angular values (hypolordosis) causes the stress falling. Key words. Stress-strain state, transpedicular fixation, lumbar spine, segmental lordosis, total lordosis, finite element method, equal tensions, geometric modelling.

Мета. Вивчити напружено-деформований стан елементів поперекового відділу хребта людини за умов застосування транспедикулярної системи з урахуванням різних кутових величин сегментарного і тотального поперекового лордозу. Методи. Для комп'ютерного моделювання напружено-деформованого стану елементів поперекового відділу хребта людини після проведення моно- та полісегментарної фіксації використано продукт Workbench, а для побудови параметричних тривимірних геометричних моделей — систему автоматизованого проєктування SolidWorks. Вивчено 4 групи рішень, які відрізнялись за кутовими величинами сегментарного і тотального поперекового лордозу. У кожній групі розглянуто 11 моделей, що описують поперекові сегменти після проведення моно- та полісегментарної фіксації за умов різних конфігурацій сагітального контуру поперекового відділу хребта. Результати. Виявлено, що максимальні напруження кіркової кістки концентруються в базовому L_V хребці за «патологічного» міжхребцевого диска L_V–S у групі пацієнтів із гіперлордозом. У випадку полісегментарної фіксації L_I–S виникає перерозподіл напружень на кіркову кістку всіх хребців, але максимальних значень вони набувають у тілах L_V і S хребців, лише в групі з гіполордозом ці напруження мінімальні. Максимальні напруження завжди припадали на вищерозташований міжхребцевий диск за умов транспедикулярної фіксації. Найбільше зростання напруження на хрящ дуговідросткових суглобів сегмента L_{IV}–L_V визначено в разі фіксації сегмента L_V–S за гіперлордозу. Максимальні напруження для стрижнів виявлено в групі з гіперлордозом і полісегментарною фіксацією L_I–S, для гвинтів — у L_V, L_{IV}, L_{III} хребцях за фіксації у всіх групах, окрім випадку з гіполордозом. Висновки. Збільшення кутових значень (гіперлордоз), які описують сегментарний і тотальний поперековий лордоз, призводить до підвищення напружень в елементах фіксувальної конструкції та структурах хребтових рухових сегментів і, навпаки, зменшення кутових значень (гіполордоз) спричинює зменшення напружень.

Key words. Stress-strain state, transpedicular fixation, lumbar spine, segmental lordosis, total lordosis, finite element method, equal tensions, geometric modelling

Introduction

The study of the stress-strain state of biological and biomechanical systems by analytical methods is impossible, because the geometric shape of the elements of the systems is quite complex to describe. Because of this, methods of discretization of complex geometric shapes are used, in particular, the finite element method [1].

Abnormalities of the lumbosacral spine are determined in more than 60 % of the total population [2]. Clinical manifestations can vary widely and depend on the segment, department and sagittal contour of the spine. Patients have a wide range of problems from mild symptoms to significant pain and severe disability. Great attention is paid to the sagittal contour of the spine and its relationship to the pelvis due to the established close correlation of curvature of the spine in the sagittal plane with disability and quality of life of the patient [3]. In fact, the assumption of error during the correction of the sagittal contour (i. e. the presence of a problem in the sagittal plane) is an independent predictor of negative results in almost all cases of spinal abnormalities in adults: scoliosis [4], spinal deformities in the sagittal plane [5], any degenerative disorder of the spine without deformity [6]. Surgical treatment of patients using transpedicular structures is used for a wide range of diseases, from degenerative disorders to significant debilitating deformities. That is why today many adult patients undergo correction or stabilization of the spine. Efforts have been made in recent decades to expand knowledge in this area, including biomechanical research. It has been shown that volumetric operations that disturb the balance of the spine in the sagittal plane, lead to unacceptably high rates of poor results and revision interventions [7–9]. In turn, increasing the efficiency of transpedicular fixation requires knowledge of biomechanical conditions of functioning of the elements of the vertebral motor segments (VMS) and their components (bone tissue of vertebral bodies, intervertebral disc, articular cartilage of the arcuate joints) under different configurations of the sagittal transpedicular configuration. In the literature, we found information on the nature of VMS loads separately for each type of connective tissue [10], but without the use of transpedicular construction. A similar study was also conducted [11], but without taking into account the conditions of different configurations of the sagittal contour of the lumbar lordosis. Further successful correction of spinal deformity or stabilization requires theoretical knowledge on load distribution on bone and cartilage tissue of anterior and posterior support structures of the VMS, as well as on rods and transpedicular screws in different variants of the sagittal contour of the lumbar spine in the case of mono- and polysegmental transpedicular fixation.
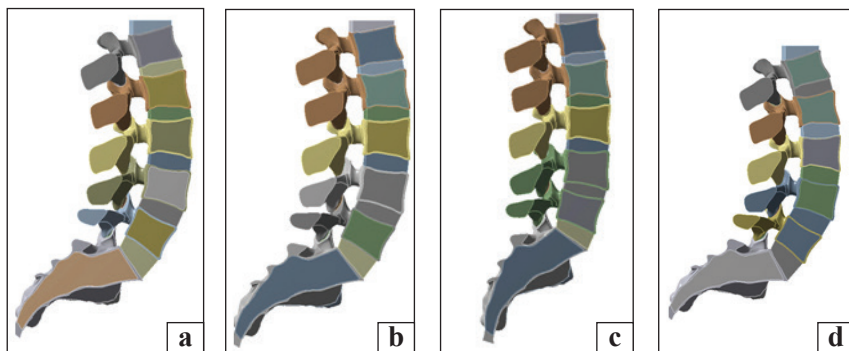
The purpose of the study: to evaluate the stress-strain state of the elements of the human lumbar spine under the conditions of transpedicular system, taking into account different angular values of segmental and total lumbar lordosis.
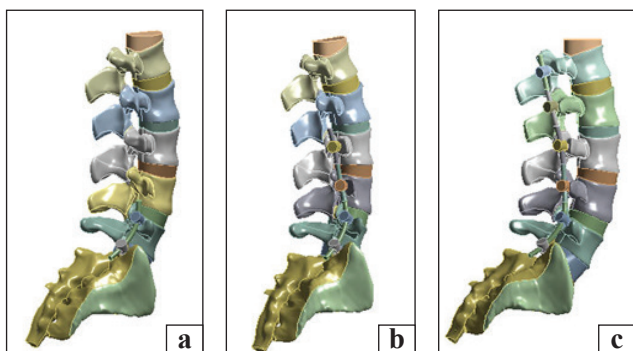
Material and methods

The study was carried out within the research work of the State Institution «Professor M. I. Sytenko Institute of Abnormalities of the Spine and Joints of the National Academy of Medical Sciences of Ukraine» «To study the main errors and complications of transpedicular fixation in spinal surgery and to develop measures for their prevention and treatment», state registration number 0118U006949.

Ansys Workbench was used for computer modeling of the stress-strain state of elements of the biomechanical system, which describes the lumbar motor segment of a person after mono- and polysegmental fixation taking into account the conditions of different configurations of the sagittal contour of the lumbar spine [12]. This software and calculation complex makes it possible to perform calculations using the finite element model method. The computer center of computer modeling «Tenzor» of the NTU «Kharkiv Polytechnic Institute», which owns the computer cluster «POLYTECHNIC-125», is equipped with this software complex. The center was involved on the basis of a cooperation agreement between the «Professor M. I. Sytenko Institute of Abnormalities of the Spine and Joints of the National Academy of Medical Sciences of Ukraine» and the National Technical University «Kharkiv Polytechnic Institute».

L_I–L_V and S (sacrum) vertebrae are included to build a finite element model. Computational models include vertebrae, intervertebral discs and cartilage of the arcuate joints. They are also supplemented by an additional element for correct load transfer. The structural division into cortical and spongy bone tissues was taken into account during the construction of vertebral models. The study created four calculation groups that describe the lumbar spine.

Fig. 1. Geometric models of the calculation group: a) the first (scheme 1.1); b) the second (scheme 2.1); c) the third (scheme 3.1); d) the fourth (scheme 4.1)

Fig. 2. Geometric models 1.7 (a), 1.9 (b) and 1.11 (c) of calculation schemes

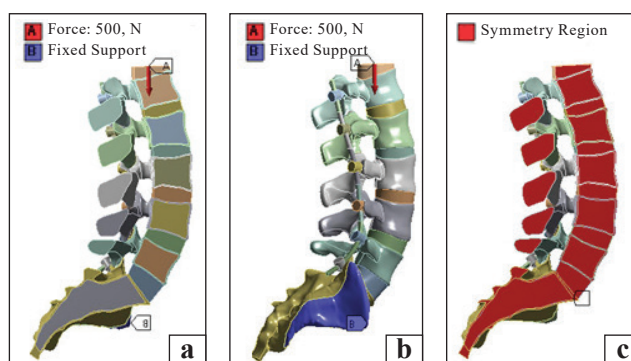**Fig. 3.** Finite element model of the calculation scheme 1.11

The differences between the calculation schemes were the angular magnitudes of segmental and total lumbar lordosis [13]. The first two calculation groups described the models of the lumbar region according to the indicators obtained by M. Bernhardt et al. [14]. The third and fourth groups analyzed the abnormal changes of segmental and total lumbar lordosis in the direction of decrease and increase, respectively. It was assumed that the normal values of segmental and total lumbar lordosis correspond to the first and second calculation groups.

Fig. 1 shows geometric models of four calculation groups, which describe the intact state of the lumbar spine (calculation schemes 1.1, 2.1, 3.1, 4.1).

Each considered calculation group consisted of 11 calculation schemes, which described the various condition of the lumbar spine, namely: intact, damaged and using the transpedicular system. The latter two analyzed different segments of the lumbar spine. Table 1 shows a description of the calculation schemes.

Fig. 2 shows a geometric model on the example of calculation scheme 1.11 from the first calculation group (a model that describes the lumbar spine with a transpedicular system) in some types of geometric model on the example of calculation schemes 1.7, 1.9 and 1.11.

Table 2 demonstrates the values of segmental and total lumbar lordosis for all calculation groups [11].

Fig. 4. Schemes of loading (a), fixing (b) and conditions of symmetry (c) (calculation scheme 1.11)

Within the framework of this study, the physical and mechanical properties of the cortical and spongy bones, cartilage of the arcuate joint, «damaged» and intact intervertebral disc are used, which are given in Table 3 [1, 10, 11, 13].

The construction of combined finite-element models took place using elements of different types, namely: 10-node tetrahedron (SOLID187), 20-node cubic element (SOLID186). The constructed finite-element models numbered about 600 thousand elements with 1.2 million nodes. Fig. 3 shows a finite element model for the first calculation scheme.

Thus, a high approximation of the stress-strain state during calculations can be obtained through

Table 1

Description of calculation schemes

Calculation group	Calculation scheme	Description
1	1.1	Intact state
	1.2	«Damaged» intervertebral discs L_V–S
	1.3	«Damaged» intervertebral discs L_{IV}–S
	1.4	«Damaged» intervertebral discs L_{III}–S
	1.5	«Damaged» intervertebral discs L_{II}–S
	1.6	«Damaged» intervertebral discs L_I–S
	1.7	«Damaged» intervertebral disc and transpedicular system L_V–S
	1.8	«Damaged» intervertebral disc and transpedicular system L_{IV}–S
	1.9	«Damaged» intervertebral disc and transpedicular system L_{III}–S
	1.10	«Damaged» intervertebral disc and transpedicular system L_{II}–S
	1.11	«Damaged» intervertebral disc and transpedicular system L_I–S
2	2.1	Intact state
	2.2	«Damaged» intervertebral discs L_V–S
	2.3	«Damaged» intervertebral discs L_{IV}–S
	2.4	«Damaged» intervertebral discs L_{III}–S
	2.5	«Damaged» intervertebral discs L_{II}–S
	2.6	«Damaged» intervertebral discs L_I–S
	2.7	«Damaged» intervertebral disc and transpedicular system L_V–S
	2.8	«Damaged» intervertebral disc and transpedicular system L_{IV}–S
	2.9	«Damaged» intervertebral disc and transpedicular system L_{III}–S
	2.10	«Damaged» intervertebral disc and transpedicular system L_{II}–S
	2.11	«Damaged» intervertebral disc and transpedicular system L_I–S
3	3.1	Intact state
	3.2	«Damaged» intervertebral discs L_V–S
	3.3	«Damaged» intervertebral discs L_{IV}–S
	3.4	«Damaged» intervertebral discs L_{III}–S
	3.5	«Damaged» intervertebral discs L_{II}–S
	3.6	«Damaged» intervertebral discs L_I–S
	3.7	«Damaged» intervertebral disc and transpedicular system L_V–S
	3.8	«Damaged» intervertebral disc and transpedicular system L_{IV}–S
	3.9	«Damaged» intervertebral disc and transpedicular system L_{III}–S
	3.10	«Damaged» intervertebral disc and transpedicular system L_{II}–S
	3.11	«Damaged» intervertebral disc and transpedicular system L_I–S
4	4.1	Intact state
	4.2	«Damaged» intervertebral discs L_V–S
	4.3	«Damaged» intervertebral discs L_{IV}–S
	4.4	«Damaged» intervertebral discs L_{III}–S
	4.5	«Damaged» intervertebral discs L_{II}–S
	4.6	«Damaged» intervertebral discs L_I–S
	4.7	«Damaged» intervertebral disc and transpedicular system L_V–S
	4.8	«Damaged» intervertebral disc and transpedicular system L_{IV}–S
	4.9	«Damaged» intervertebral disc and transpedicular system L_{III}–S
	4.10	«Damaged» intervertebral disc and transpedicular system L_{II}–S
	4.11	«Damaged» intervertebral disc and transpedicular system L_I–S

Table 2

Values of segmental and total lumbar lordosis (degree)

Vertebral segment	Calculation group			
	first	second	third	fourth
L_I–L_{II}	4.0	1.5	1.2	6.4
L_{II}–L_{III}	7.0	7.0	4.4	9.9
L_{III}–L_{IV}	13.0	1.3	4.0	16.0
L_{IV}–L_V	20.0	16.5	14.5	21.1
L_V–S	28.0	24.6	19.2	27.4
L_I–S	72.0	60.9	43.3	80.8

Table 3

Physico-mechanical characteristics of materials

Material	Young's modulus E, (МПа)	Poisson's ratio v
Cortical bone	10 000.0	0.30
Spongy bone	450.0	0.20
Cartilage of the zygapophysial joint	10.6	0.49
Intervertebral disc	4.2	0.45
Titanium	102 000.0	0.30
«Damaged» intervertebral disc	1.6	0.45

Table 4

Maximum equivalent stresses (MPa) for the cortical bone

Vertebra	Calculation scheme										
	1	2	3	4	5	6	7	8	9	10	11
1st calculation group											
L_I	43.00	78.76	92.18	99.89	104.78	113.94	12.20	11.49	10.33	9.58	27.80
L_{II}	31.39	59.41	69.93	75.97	79.83	79.09	10.14	7.28	9,13	70.00	65.00
L_{III}	16.21	28.49	33.31	36.13	36.04	35.81	14.10	13.09	10.05	7.96	7.52
L_{IV}	39.43	40.12	44.62	44.85	44.93	45.04	28.34	80.00	79.55	60.00	66.40
L_V	73.63	139.59	138.28	137.65	137.31	136.80	100.00	80.00	80.00	70.00	70.00
S	25.16	27.81	27.65	27.57	27.53	27.47	133.79	104.23	109.90	103.03	97.38
2nd calculation group											
L_I	35.86	59.22	69.17	77.21	82.32	88.67	7.91	7.72	7.79	7.83	20.39
L_{II}	35.33	59.67	70.04	78.41	83.64	83.44	8.85	7.72	9.11	80.00	75.00
L_{III}	15.67	26.11	30.56	34.18	34.06	33.91	11.05	11.11	13.26	10.34	9.88
L_{IV}	32.70	33.34	37.06	37.20	37.30	37.41	24.74	88.40	72.75	68.43	64.39
L_V	46.15	86.49	85.54	85.06	84.80	84.54	50.00	88.82	85.91	80.30	75.11
S	26.77	31.93	31.67	31.48	31.38	31.28	124.26	110.35	107.16	101.77	96.67
3rd calculation group											
L_I	12.51	21.71	26.01	30.76	34.57	40.00	7.48	7.37	7.49	7.58	38.49
L_{II}	7.27	13.87	16.87	20.17	22.85	22.60	6.94	6.97	8.25	50.00	94.25
L_{III}	10.48	10.63	11.92	14.15	14.07	13.96	8.79	9.03	7.80	6.23	15.34
L_{IV}	20.11	20.34	23.75	23.97	24.04	24.13	15.37	47.62	44.49	46.14	100.00
L_V	28.92	47.75	47.61	47.31	47.10	46.88	26.99	28.54	28.22	26.78	52.13
S	13.28	15.25	15.18	15.12	15.08	15.03	64.86	63.17	62.40	50.87	33.85
4th calculation group											
L_I	48.99	80.44	93.44	100.94	106.10	114.51	11.09	14.38	14.65	13.68	37.25
L_{II}	48.20	80.71	94.14	101.89	107.25	106.52	9.49	8.25	8.82	75.00	100.00
L_{III}	22.56	36.83	42.73	46.20	46.07	45.84	15.34	15.76	12.43	10.83	8.76
L_{IV}	41.88	42.61	42.45	42.78	42.88	43.01	31.21	60.00	77.01	69.99	53.01
L_V	84.48	146.84	145.20	144.47	144.05	143.55	100.00	80.00	90.50	60.00	65.92
S	26.80	30.11	29.86	29.74	29.68	29.60	100.00	60.00	99.51	70.00	78.67

the use of two different types of elements in finite element models.

With the help of the appropriate force, the required load is reproduced. The force applied in the vertical direction was 500 N (i. e. 50 kg). This value was obtained taking into account the symmetry in the sagittal plane. Part of the sacral zone S of the vertebra was specially allocated for fixation. Fig. 4 illustrates the schemes of loading, fixing and conditions of symmetry in the sagittal area on the example of the calculation scheme 1.11.

Results and their discussion

Based on the results of the studies of four calculation groups, the maximum equivalent stresses by von Mises and total displacements for the studied lumbar segment of biological and biomechanical systems were determined.

Diagrams with stress indices by von Mises of the cortical bone for all calculation groups are shown in Fig. 5–8 (Table 4), intervertebral discs and cartilage of the arcuate joints in Fig. 9–12 (Table 5) and 13–16 (Table 6), respectively.

Diagrams with maximum equivalent stresses by von Mises in the elements of the transpedicular system are shown in Fig. 17–23 (Table 7), namely for rods and screws located in the S, LV–LI vertebrae.

The indicators that correspond to the maximum total displacement obtained for all calculation schemes are shown in the diagram in Fig. 24 (Table 8).
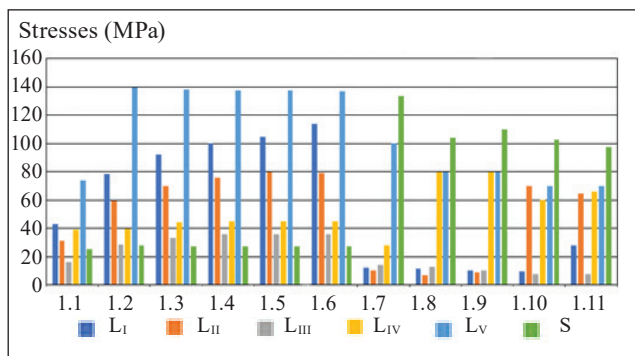
Given that the first and second calculation groups describe models with close values of angles, which outline the normal values of segmental and total lumbar lordosis, the obtained values of maximum equivalent stresses and total displacements are close.

In the first calculation group (with normal lordosis), the maximum equivalent stresses on the cortical bone of the L_V vertebra are 140 MPa for the «abnormal» intervertebral disc L_V–S (Fig. 5). Compared with the fourth calculation group (with hyperlordosis), these stresses on the cortical bone L_V of the vertebrae increased to 147 MPa (Fig. 8). This can
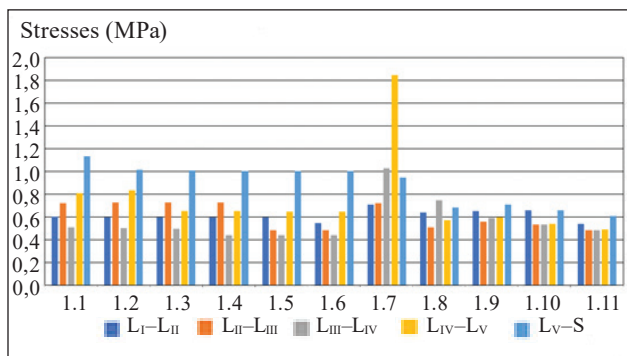
Table 5

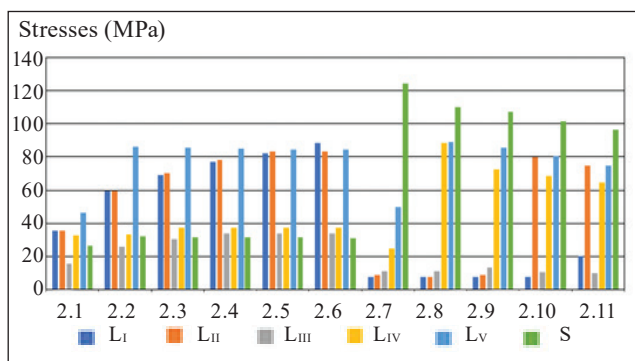**Maximum equivalent stresses (MPa) for intervertebral discs**

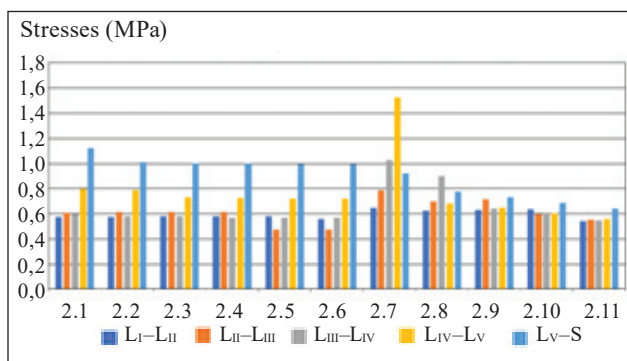| Spine segment	Calculation scheme										
	1	2	3	4	5	6	7	8	9	10	11
1st calculation group											
L_I–L_{II}	0.60	0.60	0.60	0.60	0.60	0.55	0.71	0.64	0.65	0.66	0.54
L_{II}–L_{III}	0.72	0.73	0.73	0.73	0.48	0.48	0.72	0.51	0.56	0.53	0.48
L_{III}–L_{IV}	0.51	0.50	0.50	0.44	0.44	0.44	1.03	0.75	0.59	0.53	0.48
L_{IV}–L_V	0.81	0.84	0.66	0.65	0.65	0.65	1.85	0.57	0.60	0.54	0.49
L_V–S	1.14	1.02	1.01	1.01	1.00	1.00	0.95	0.69	0.71	0.66	0.61
2nd calculation group											
L_I–L_{II}	0.58	0.58	0.58	0.58	0.58	0.56	0.65	0.62	0.63	0.64	0.54
L_{II}–L_{III}	0.61	0.61	0.61	0.62	0.47	0.47	0.79	0.70	0.71	0.60	0.55
L_{III}–L_{IV}	0.60	0.58	0.58	0.57	0.57	0.57	1.03	0.90	0.64	0.59	0.55
L_{IV}–L_V	0.80	0.79	0.73	0.72	0.72	0.72	1.53	0.68	0.65	0.60	0.56
L_V–S	1.12	1.01	1.00	1.00	1.00	0.99	0.92	0.77	0.73	0.69	0.64
3rd calculation group											
L_I–L_{II}	0.62	0.62	0.62	0.62	0.62	0.60	0.61	0.62	0.63	0.64	0.53
L_{II}–L_{III}	0.51	0.51	0.51	0.51	0.57	0.57	0.62	0.64	0.67	0.64	0.48
L_{III}–L_{IV}	0.61	0.61	0.61	0.66	0.66	0.65	0.81	0.82	0.72	0.68	0.40
L_{IV}–L_V	0.73	0.74	0.58	0.58	0.58	0.58	0.90	0.59	0.58	0.55	0.29
L_V–S	0.79	0.75	0.75	0.75	0.74	0.74	0.64	0.61	0.60	0.57	0.31
4th calculation group											
L_I–L_{II}	0.62	0.62	0.62	0.62	0.62	0.52	0.68	0.65	0.64	0.65	0.48
L_{II}–L_{III}	0.61	0.61	0.61	0.61	0.39	0.39	0.73	0.64	0.59	0.49	0.40
L_{III}–L_{IV}	0.50	0.50	0.50	0.40	0.40	0.39	1.01	0.85	0.47	0.43	0.32
L_{IV}–L_V	0.84	0.82	0.73	0.73	0.73	0.72	1.64	0.69	0.47	0.49	0.37
L_V–S	1.32	1.21	1.20	1.20	1.19	1.19	1.03	0.90	0.72	0.68	0.54

Fig. 5. Maximum equivalent stresses (MPa) for the cortical bone — the first calculation group
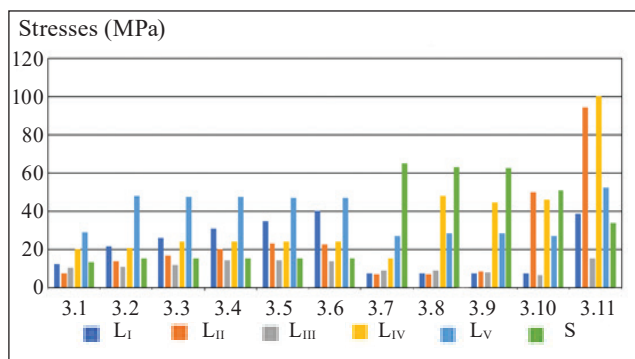

Fig. 9. Maximum equivalent stresses (MPa) for intervertebral discs — the first calculation group
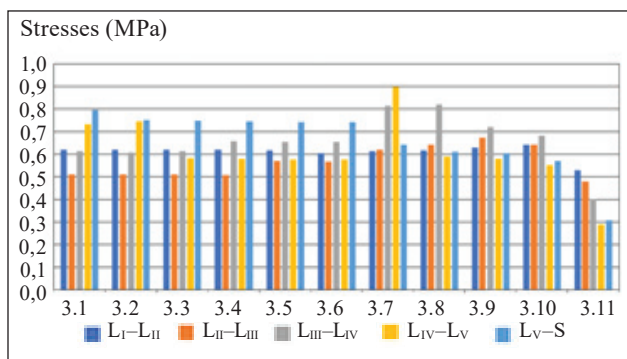

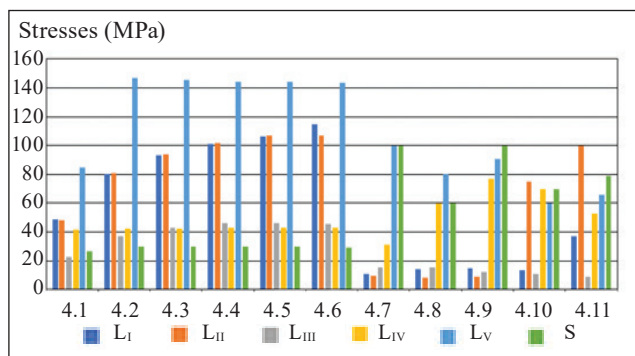**Fig. 6.** Maximum equivalent stresses (MPa) for the cortical bone — the second calculation group

Fig. 10. Maximum equivalent stresses (MPa) for intervertebral discs — the second calculation group
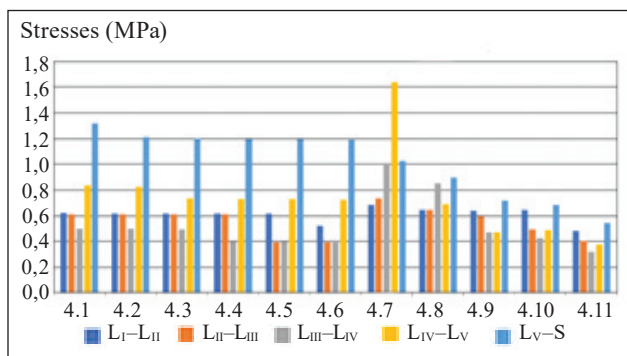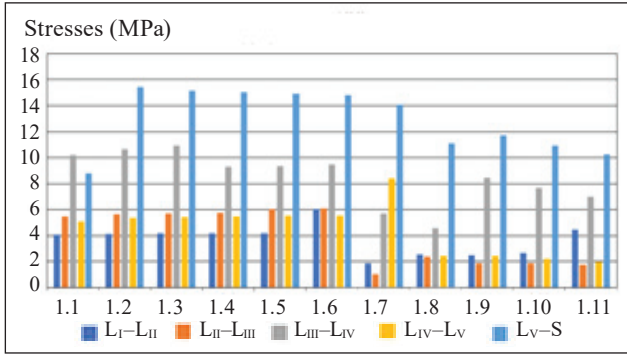

Fig. 7. Maximum equivalent stresses (MPa) for the cortical bone — the third calculation group

Fig. 11. Maximum equivalent stresses (MPa) for intervertebral discs — the third calculation group
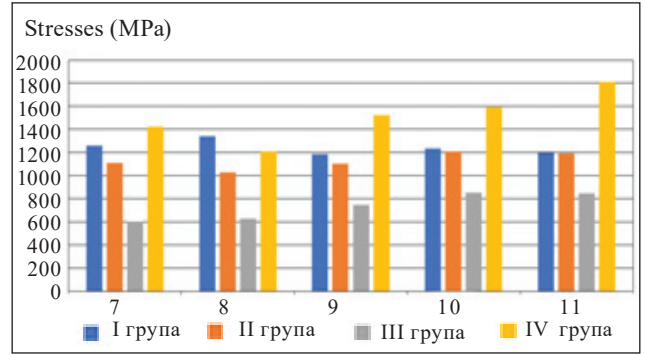

Fig. 8. Maximum equivalent stresses (MPa) for the cortical bone — the fourth calculation group
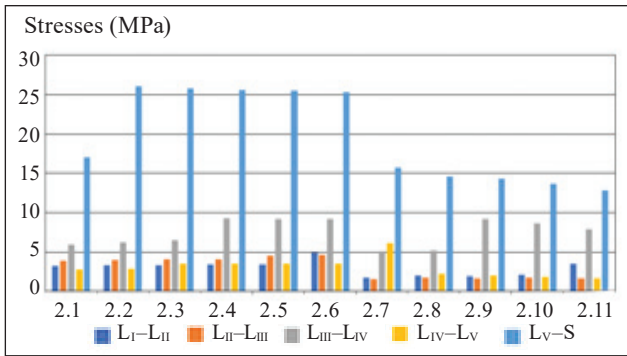

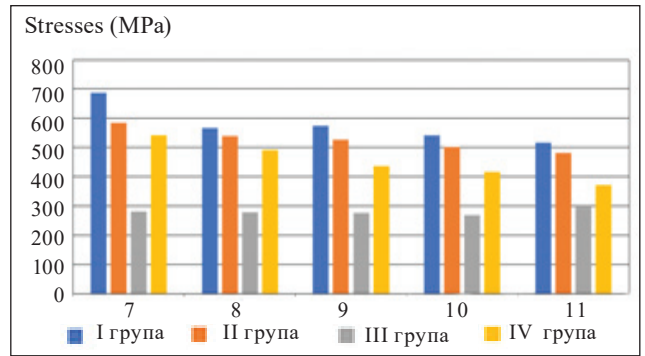**Fig. 12.** Maximum equivalent stresses (MPa) for intervertebral discs — the fourth calculation group

Fig. 13. Maximum equivalent stresses (MPa) for the cartilage of the arcuate joints — the first calculation group
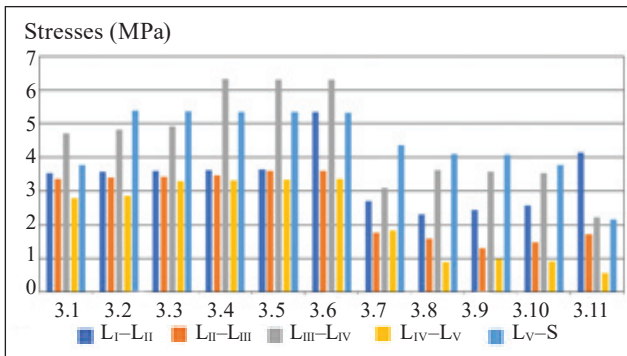

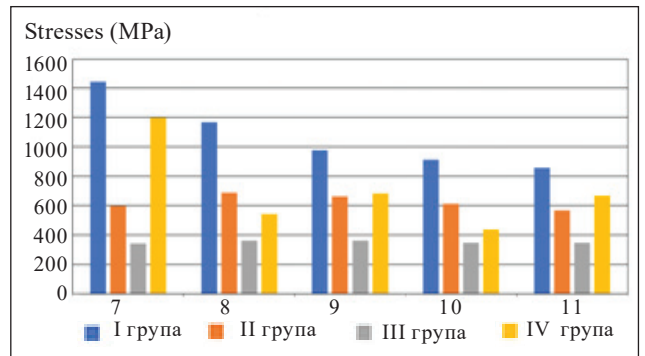**Fig. 17.** Maximum equivalent stresses (MPa) for the rod

Fig. 14. Maximum equivalent stresses (MPa) for the cartilage of the arcuate joints — the second calculation group
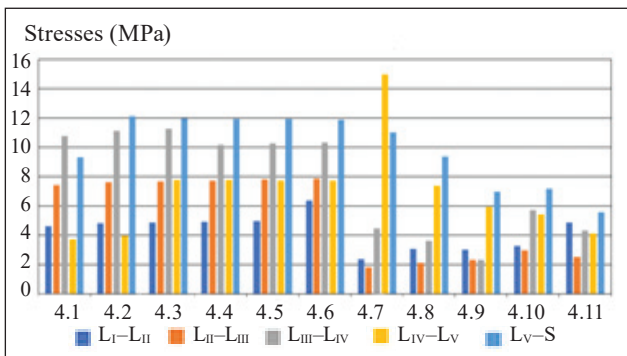

Fig. 18. Maximum equivalent stresses (MPa) for the screw (S)
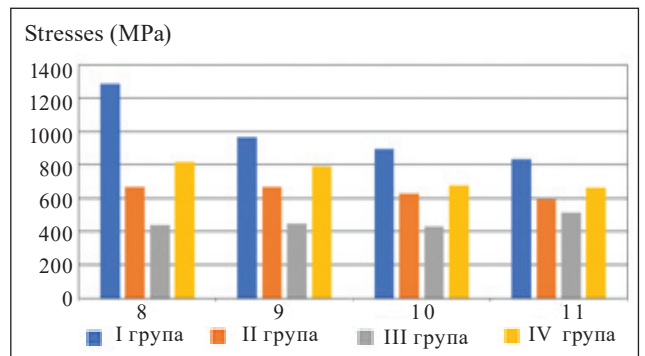

Fig. 15. Maximum equivalent stress (MPa) for the cartilage of the arcuate joints — the third calculation group

Fig. 19. Maximum equivalent stresses (MPa) for the screw (L_V)

Fig. 16. Maximum equivalent stresses (MPa) for the cartilage of the arcuate joints — the fourth calculation group

Fig. 20. Maximum equivalent stresses (MPa) for the screw (L_{IV})

Table 6

Maximum equivalent stresses (MPa) for the cartilage of the zygapophysial joint

Spine segment	Calculation scheme										
	1	2	3	4	5	6	7	8	9	10	11
1st calculation group											
L_I–L_{II}	4.08	4.15	4.18	4.19	4.20	6.05	1.91	2.57	2.50	2.68	4.45
L_{II}–L_{III}	5.51	5.66	5.72	5.76	6.04	6.08	1.05	2.42	1.91	1.90	1.77
L_{III}–L_{IV}	10.23	10.65	10.92	9.31	9.39	9.46	5.73	4.58	8.47	7.70	7.02
L_{IV}–L_V	5.08	5.37	5.43	5.48	5.52	5.57	8.39	2.42	2.47	2.21	2.00
L_V–S	8.80	15.43	15.17	15.03	14.95	14.84	14.08	11.09	11.75	10.95	10.25
2nd calculation group											
L_I–L_{II}	3.23	3.32	3.36	3.40	3.42	4.96	1.80	2.04	1.95	2.10	3.57
L_{II}–L_{III}	3.93	4.04	4.09	4.09	4.60	4.62	1.60	1.78	1.69	1.74	1.65
L_{III}–L_{IV}	5.95	6.26	6.48	9.27	9.20	9.18	5.16	5.22	9.18	8.68	7.92
L_{IV}–L_V	2.83	2.88	3.53	3.54	3.55	3.56	6.17	2.25	2.01	1.85	1.68
L_V–S	17.07	26.06	25.80	25.59	25.48	25.36	15.73	14.66	14.29	13.64	12.87
3rd calculation group											
L_I–L_{II}	3.54	3.58	3.60	3.62	3.64	5.34	2.70	2.31	2.45	2.57	4.14
L_{II}–L_{III}	3.36	3.41	3.43	3.46	3.60	3.61	1.77	1.59	1.30	1.48	1.73
L_{III}–L_{IV}	4.71	4.82	4.93	6.32	6.31	6.30	3.10	3.62	3.57	3.53	2.23
L_{IV}–L_V	2.78	2.86	3.29	3.32	3.34	3.36	1.82	0.89	0.98	0.93	0.58
L_V–S	3.77	5.40	5.38	5.36	5.34	5.33	4.36	4.11	4.07	3.78	2.15
4th calculation group											
L_I–L_{II}	4.65	4.83	4.90	4.94	4.96	6.40	2.40	3.07	3.03	3.30	4.89
L_{II}–L_{III}	7.43	7.61	7.69	7.73	7.84	7.88	1.85	2.13	2.33	2.96	2.52
L_{III}–L_{IV}	10.76	11.14	11.28	10.20	10.27	10.34	4.46	3.63	2.33	5.71	4.32
L_{IV}–L_V	3.71	4.00	7.78	7.77	7.75	7.72	14.97	7.37	5.92	5.45	4.12
L_V–S	9.32	12.10	12.00	11.94	11.91	11.87	11.01	9.38	6.98	7.18	5.59

lead to an increase in the load on the adjacent segment in general and can be regarded as the beginning of the cascade to the development of the load on the adjacent segment.

If we consider options for transpedicular fixation, then using a monosegmental structure L_V–S and «damaged» disc at this level increases the equivalent stress on the cortical bone L_V and S vertebrae (from 100 to 134 MPa) in groups with normal condition and hyperlordosis. In the case of polysegmental fixation L_I–S, there is a redistribution of stress on the cortical bone of all vertebrae, but the maximum stresses (from 60 to 98 MPa) occur on the L_V and S vertebrae in almost all calculation groups (Fig. 5, 6, 8). Only in the group with hypolordosis these stresses are minimal — 33 and 52 MPa (Fig. 7).

Considering the maximum equivalent stresses on the intervertebral disc, we found an increase in the load on the upper disc under conditions of transpedicular fixation.

In particular, in the first calculation group with hypolordosis in the scheme with a «damaged» L_V–S disc with transpedicular fixation of this segment, the stress on the intervertebral disc L_{IV}–L_V increases to 0.90 MPa compared to the intact state (0.73 MPa) (Fig. 9–11). The tension on the adjacent intervertebral disc L_{IV}–L_V increases significantly when the L_V–S segment is fixed in the group with hyperlordosis (Fig. 12). The data obtained emphasize the relationship between the factors of load redistribution in the adjacent segments.

The maximum increase in the stress on the cartilage of the arcuate joints of the L_{IV}–L_V segment up to 15 MPa was determined in the case of fixation of the L_V–S VMS in the fourth calculation group with hyperlordosis. In other groups, the obtained values do not allow to assert a clear pattern of their changes (Fig. 13–16).

During the study, the maximum values of equivalent spongy bone stresses for calculation schemes 1 and 7–11 did not exceed 10 MPa, but for schemes
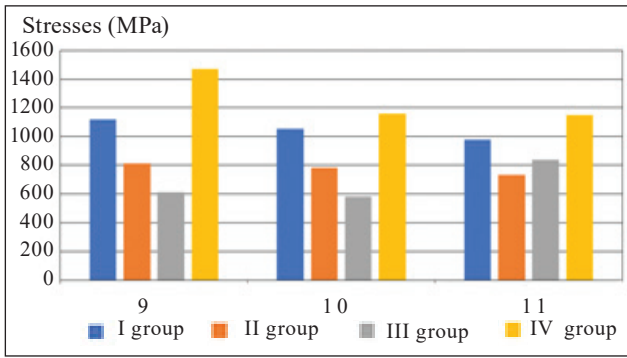
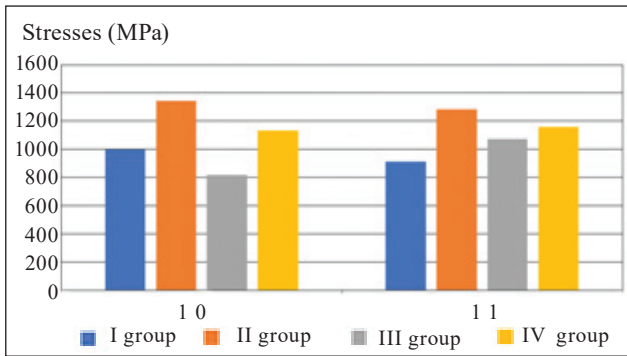**Fig. 21.** Maximum equivalent stresses (MPa) for the screw (L$_{III}$)

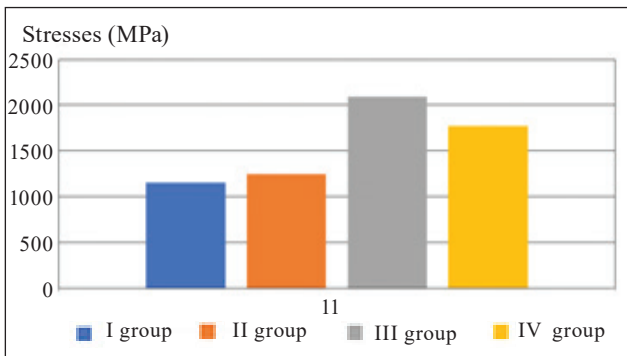**Fig. 22.** Maximum equivalent stresses (MPa) for the screw (L$_{II}$)

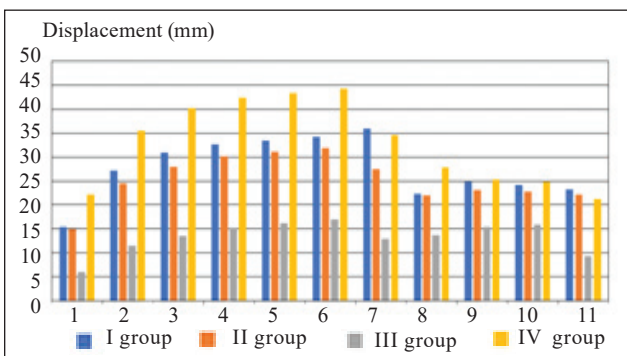**Fig. 23.** Maximum equivalent stresses (MPa) for the screw (L$_{I}$)

Fig. 24. Maximum full displacements

<div style="text-align:right">*Table 7*</div>

**Maximum equivalent stresses (MPa)
for rods and screws**

Calculation group	Calculation scheme				
	7	8	9	10	11
Rod					
1	1263.10	1343.50	1184.50	1236.80	1196.20
2	1112.80	1030.00	1106.80	1213.60	1191.90
3	601.65	629.20	748.00	850.96	848.60
4	1426.40	1208.20	1525.70	1591.40	1813.90
Screw (S)					
1	687.51	566.79	574.23	542.14	515.64
2	585.09	539.23	525.76	502.55	480.44
3	281.26	278.67	276.80	268.82	297.26
4	540.60	492.48	437.63	416.83	372.02
Screw (L$_V$)					
1	1444.40	1167.30	976.99	910.57	855.61
2	597.35	687.39	660.01	611.95	567.15
3	339.03	363.26	361.08	348.40	344.00
4	1198.50	543.21	684.00	437.04	666.56
Screw (L$_{IV}$)					
1	—	1286.40	967.71	894.58	834.17
2	—	669.01	666.61	627.99	591.19
3	—	439.17	448.89	430.40	513.44
4	—	816.33	791.87	674.80	660.97
Screw (L$_{III}$)					
1	—	—	1121.50	1053.80	979.86
2	—	—	812.24	781.58	733.61
3	—	—	614.14	582.73	841.07
4	—	—	1468.20	1160.80	1148.30
Screw (L$_{II}$)					
1	—	—	—	997.95	912.90
2	—	—	—	1345.90	1282.70
3	—	—	—	816.46	1075.30
4	—	—	—	1134.30	1158.70
Screw (L$_I$)					
1	—	—	—	—	1150.60
2	—	—	—	—	1247.40
3	—	—	—	—	2092.30
4	—	—	—	—	1773.80

2–6, which correspond to the «abnormal» condition without transpedicular fixation, the values are critically close to the spongy bone strength — 16–22 MPa [15]. The described tendency was observed in the process of studying the maximum equivalent stresses of cortical bones corresponding to the L$_V$ vertebrae of the calculation schemes 2–6, but they did not exceed the strength limit — 160 MPa [16].

Table 8

Maximum full displacements

Calculation group	Calculation scheme										
	1	2	3	4	5	6	7	8	9	10	11
1	15.40	27.26	31.00	32.67	33.40	34.26	35.99	22.28	24.78	24.17	23.29
2	14.91	24.50	27.95	30.13	31.11	31.83	27.52	22.00	23.13	22.90	22.20
3	6.05	11.60	13.57	15.25	16.22	17.07	12.99	13.80	15.46	15.94	9.41
4	22.17	35.58	40.24	42.34	43.34	44.32	34.61	27.87	25.26	24.85	21.31

Assessment of the maximum equivalent stresses of the rod values for the first and second calculation groups (describes the normal angles of segmental and total lordosis) showed stresses close to the values of the fourth (gives the largest angles of segmental and total lumbar lordosis) — 1,100–1,800 MPa. The maximum stress of 1,800 MPa falls on the rod in the fourth group, calculation scheme 11 (with hyperlordosis and polysegmental fixation L_I–S). The lowest values of the maximum equivalent stresses (600–850 MPa) were determined only in the third group, which describes the reduced angles of segmental and total lordosis (Fig. 17). The noted tendency is most pronounced in the case of studying the maximum total displacements (Fig. 24). Analysis of their values obtained in the elements of the transpedicular system revealed indicators close to the strength limit of 600–1,000 MPa [17].

After examining the obtained values of the maximum equivalent stresses for the screws, the largest were recorded in the L_V vertebra under the conditions of fixation in all calculation groups, except the third (hypolordosis). The same stresses were observed in the L_{IV} vertebra. This is probably due to the fact that 50 % of total lordosis falls on the corners of the intervertebral segments L_{IV}–L_V, L_V–S. Also, the maximum equivalent stress on the screw was observed in the L_{III} vertebra in the group with hyperlordosis, and this is expected because it is located at the apex of the bend of the enlarged lordosis (Fig. 18–23). However, in the calculation scheme 11, where the values of stresses in the screw, which is located in the L_I vertebra, are the largest in all calculation groups, as well as in the group with hypolordosis, they are maximum. This is most likely due to the fact that this vertebra is the last in the elaborated finite element model, on top of it an additional element is created for the correct transfer of load. That is, with high probability these values have an error and, perhaps, in the case of building a model with Th_{XI}, Th_{XII} vertebral bodies, these values will be changed.

Conclusions

Changes in angular parameters (hypo- and hyperlordosis), which describe segmental and total lumbar lordosis, significantly change the stress-strain state. The use of a transpedicular system leads to the stabilization of the «damaged» segment, as well as to the redistribution and reduction of stresses. An increase in angular values (hyperlordosis), which describe segmental and total lumbar lordosis, causes an increase in emerging stresses in the elements of biological and biomechanical systems and, conversely, a decrease in angular values (hypolordosis) leads to a decrease in stress. These conclusions are consistent in the case of full displacements. Based on the results of the research, parametric models were constructed, which describe different angular values of segmental and total lumbar lordosis, as well as various states of the lumbar spine, without and taking into account the transpedicular system.

Conflict of interest. The authors declare the absence of conflict of interest.

References

1. Zienkiewicz O. C. The finite element method: its basis and fundamentals / O. C. Zienkiewicz, R. L. Taylor, J. Z. Zhu. — Amsterdam ; Heidelberg : Butterworth-Heinemann, 2006. — 631 p.
2. Roussouly P. Sagittal plane deformity: an over-view of interpretation and management / P. Roussouly, C. Nnadi // European Spine Journal. — 2010. — Vol. 19 (11). — P. 1824–1836. — DOI: 10.1007/s00586-010-1476-9.
3. Pelvic tilt and truncal inclination: two key radiographic parameters in the setting of adults with spinal deformity / V. Lafage, F. Schwab, A. Patel [et al.] // Spine. — 2009. — Vol. 34 (17). — P. E599–E606. — DOI: 10.1097/BRS.0b013e3181aad219.
4. Risk-benefit assessment of surgery for adult scoliosis: an analysis based on patient age / J. S. Smith, C. I. Shaffrey, S. D. Glassman [et al.] // Spine. — 2011. — Vol. 36 (10). — P. 817–824. — DOI: 10.1097/BRS.0b013e3181e21783.
5. Role of pelvic incidence, thoracic kyphosis, and patient factors on sagittal plane correction following pedicle subtraction osteotomy / P. S. Rose, K. H. Bridwell, L. G. Lenke [et al.] // Spine. — 2009. — Vol. 34 (8). — P. 785–791. — DOI: 10.1097/BRS.0b013e31819d0c86.
6. The impact of sagittal balance on clinical results after posterior interbody fusion for patients with degenerative spondylolisthesis: a pilot study / K. Mi Kyung, L. Sun-Ho, K. Eun-Sang [et al.] // BMC Musculoskelet Disord. — 2001. — P. 12–69. —

DOI: 10.1186/1471-2474-12-69.

7. Jackson R. P. Radiographic analysis of sagittal plane alignment and balance in standing volunteers and patients with low back pain matched for age, sex, and size. A prospective controlled clinical study / R. P. Jackson, A. C. McManus // Spine. — 1994. — Vol. 19 (14). — P. 1611–1618. — DOI: 10.1097/00007632-199407001-00010.

8. Sagittal alignment in lumbosacral fusion: relations between radiological parameters and pain / J. Y. Lazennec, S. Ramare, N. Arafati [et al.] // European Spine Journal. — 2000. — Vol. 9 (1). — P. 47–55— DOI: 10.1007/s005860050008..

9. Implications of spinopelvic alignment for the spine surgeon / V. A. Mehta, A. Amin, I. Omeis [et al.] // Neurosurgery. — 2012. — Vol. 70 (3). — P. 707–721. — DOI: 10.1227/NEU.0b013e31823262ea.

10. Piontkovsky, V. K., Tkachuk, M. A., Veretelnyk, O. V., & Radchenko, V. O. (2018). Influence of lumbar-pelvic relations on the stress-strain state of the lumbar spine. Orthopedics, traumatology and prosthetics, 4(613), 24–30. https://doi.org/10.15674/0030-59872018424-30.

11. ANSYS Workbench [web source]. — Available from : http://www.ansys.com.

12. Mezentsev, A. A., Petrenko, D. E., Barkov, A. A., & Yaresko, A. V. (2011). Investigation of the stress-strain state of the system "implant - lumbar spine - pelvis" with different fixation options. Orthopedics, traumatology and prosthetics, (2), 37– 41. https://doi.org/10.15674/0030-59872011237-41.

13. Piontkovsky, V. K. (2019). Pathogenesis, diagnosis and surgical treatment of lumbar intervertebral disc herniation in elderly and senile patients. Diss. of Doctor in Medical Sciences. Kharkiv.

14. Bernhardt M. Segmental analysis of the sagittal plane alignment of the normal thoracic and lumbar spines and thoracolumbar junction / M. Bernhardt, K. H. Bridwell // Spine. — 1989. — Vol. 14 (7). — P. 717–721. — DOI: 10.1097/00007632-198907000-00012.

15. http://fcpir.ru/upload/iblock/879/stagesummary_corebofs 000080000kif04cm57m6em8o.pdf.

16. Kukin, I. A., Kirpichev, I. V., Maslov, L. B., & Vikhrev, S. V. (2013). Features of the strength characteristics of cancellous bone in diseases of the hip joint. Funfamental research, 7, 328–333.

17. http://metallicheckiy-portal.ru/marki_metallov/tit/VT20.

INFLUENCE OF THE SAGITTAL LUMBAR PARAMETERS ON THE STRESS-STRAIN STATE OF THE SPINAL MOTOR SEGMENTS AT TRANSPEDICULAR FIXATION

O. O. Barkov [1], O. V. Veretelnik [2], M. M. Tkachuk [2], M. A. Tkachuk [2], V. V. Veretelnik [2]

[1] Sytenko Institute of Spine and Joint Pathology National Academy of Medical Sciences of Ukraine, Kharkiv
[2] National Technical University «Kharkiv Polytechnic Institute». Ukraine

✉ Oleksandr Barkov, MD, PhD in Traumatology and Orthopaedics: a.barkov.79@gmail.com
✉ Oleg Veretelnik: veretelnyk.oleg@gmail.com
✉ Mykola Tkachuk, PhD in Tech. Sci.: tma@tmm-sapr.org
✉ Mykola A. Tkachuk, Prof. in Tech. Sci.: tma@tmm-sapr.org
✉ Victor Veretelnik, PhD in Phis.-Math.. Sci.: veretelnik.victor@gmail.com